European Journal of Medicinal Chemistry 44 (2009) 2459–2467

Contents lists available at ScienceDirect

European Journal of Medicinal Chemistry

journal homepage: http://www.elsevier.com/locate/ejmech

Original article

Photo-inducible cytotoxic and clastogenic activities of 3,6-di-substituted acridines obtained by acylation of proflavine

Yohann Benchabane [b], Carole Di Giorgio [a,*], Gérard Boyer [b], Anne-Sophie Sabatier [a], Diane Allegro [c], Vincent Peyrot [c], Michel De Méo [a]

[a] Laboratoire de Biogénotoxicologie et Mutagenèse Environnementale (EA 1784, FR 3098 – ECCOREV), Université Aix-Marseille, Faculté de Pharmacie, 27 Bd Jean Moulin, 13385 Marseille, Cedex 05, France
[b] Laboratoire HIT, case 552, (iSm2 – UMR 6263) – Université Paul Cézanne, Faculté St Jérôme, 13397 Marseille, Cedex 20, France
[c] CRO2 INSERM-U91 – Université Aix-Marseille, Faculté de Pharmacie, 27 Bd Jean Moulin, 13385 Marseille, Cedex 05, France

ARTICLE INFO

Article history:
Received 7 July 2008
Received in revised form
9 December 2008
Accepted 9 January 2009
Available online 20 January 2009

Keywords:
Proflavine derivatives
Phototoxicity
Photogenotoxicity
Micronucleus assay

ABSTRACT

The cytotoxicity and photo-enhanced cytotoxicity of a series of 18 3,6-di-substituted acridines were evaluated on both tumour CHO cells and human normal keratinocytes, and compared to their corresponding clastogenicity as assessed by the micronucleus assay.
Compounds **2f** *tert*-butyl *N*-[(6-*tert*-butoxycarbonylamino)acridin-3-yl]carbamate and **2d** *N*-[6-(pivalamino)acridin-3-yl]pivalamide displayed a specific cytotoxicity on CHO cells. These results suggested that the two derivatives could be considered as interesting candidates for anticancer chemotherapy and hypothesized that the presence of 1,1-dimethylethyl substituents was responsible for a strong non-clastogenic cytotoxicity. Compounds **2b** and **2c**, on the contrary, displayed a strong clastogenicity. They indicated that the presence of nonbranched aliphatic chains on positions 3 and 6 of the acridine rings tended to induce a significant clastogenic effect. Finally, they established that most of the acridine compounds could be photo-activated by UVA-visible rays and focussed on the significant role of light irradiation on their biological properties.

1. Introduction

Since their first discovery in the 1880s, acridines have demonstrated a broad spectrum of pharmacological properties [1]. First employed as antibacterial agents during the beginning of the twentieth century [2], they have rapidly revealed interesting antiproliferative activities against both protozoa [3] and tumour cells [4]. As a consequence, they have been extensively used in antiparasitic [3] and antitumoral [4] chemotherapy and a wide range of new acridine-derived analogues have been continuously synthesized and assessed for their pharmacological properties.

The antitumoral and anti-infectious activities of acridines are mainly related to their capacity to reversibly bind with DNA [5]. Due to their planar polycyclic structure, they have been shown to intercalate between DNA double-strands, to interfere with DNA regulatory enzymes such as topoisomerase I and II and to disrupt DNA functions in cells [6]. This DNA-intercalating activity, first demonstrated with proflavine [7], has revealed genotoxic properties leading to mutagenicity, reproductive toxicity and carcinogenicity, and has been shown to result in an increased risk of secondary tumour in patients overcoming acridine-based therapies [8,9].

The other important physicochemical property of acridines is their capacity to absorb light energy. This property allows the use of acridine chromophores in sensitive spectroscopic techniques; however it also results in a different biological behaviour of the molecules when they are exposed to light radiations as compared to their activity in the dark. As a consequence, several elements of the acridine series have exhibited photo-inducible pharmacological properties, mainly photo-toxicity, photo-bactericidal activity [10] and photo-enhanced mutagenicity [11,12].

In a preceding study, we have assessed the antileishmanial activity of eight 3,6-di-substituted analogues of proflavine and we have demonstrated that some of these compounds exerted an interesting antiparasitic activity [13]. However, we have also observed that several compounds exhibited a concomitant significant DNA-binding activity. In the present work, new acridine derivatives were produced by a new synthesis protocol, and assessed for their photo-inducible cytotoxicity against both transformed and normal cells as compared to their capacity to induce chromosomal mutations and rearrangements.

* Corresponding author.
E-mail address: Carole.Digiorgio@Pharmacie.univ-mrs.fr (C. Di Giorgio).

0223-5234/$ – see front matter © 2009 Elsevier Masson SAS. All rights reserved.
doi:10.1016/j.ejmech.2009.01.010

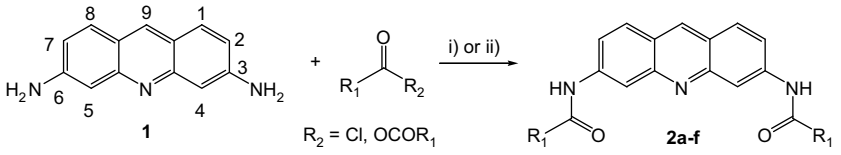

i) Pyridine, Et_3N, 1h, 80°C
ii) Acetone, K_2CO_3, 15h, rt

Comp.	R_1	Yields	MW	Molecular formula	Mp °C
2a	Me	60%	293	$C_{17}H_{15}N_3O_2$	> 260
2b	Et	65%	321	$C_{19}H_{19}N_3O_2$	> 260
2c	Pr	32%	349	$C_{21}H_{23}N_3O_2$	216
2d	tBu	74%	378	$C_{23}H_{27}N_3O_2$	158
2e	OMe	70%	325	$C_{17}H_{15}N_3O_4$	> 260
2f	OtBu	75%	410	$C_{23}H_{27}N_3O_4$	165

Compounds **2a-c**: see ref. 13

Fig. 1. Synthesis of compounds **2a**–**f**.

2. Chemistry

The preparation of symmetrical acetamides was performed using neutral proflavine **1**, which was acylated alternatively with different anhydrides and benzoyl chlorides to yield the corresponding amides as reported in Figs. 1–3. Acetone was sometimes preferred to the more toxic pyridine and allowed more favourable conditions of reaction at room temperature. However, the purification of these products was very difficult owing to their low solubility in organic solvents, and inorganic base K_2CO_3 preferred to NEt_3 to improve the technique.

First, proflavine **1** was allowed to react with different anhydrides and alkoyl chlorides to lead to the corresponding acetamides (**2a**–**f**), low to good yields were obtained (32–91%) as reported in Fig. 1. As shown in Fig. 2, different benzoyl chlorides were employed and led to diamido acridines **3a**–**i** with yields reaching 47–96%; and the 4-nitro-N-[6-(4-nitrobenzoylamino)acridin-3-yl]benzamide **3e** was reduced according to a modified procedure, using palladium under hydrogen atmosphere (3 bar) in EtOH [14]. The symmetrical bis amine **3j** was recovered with 26% yield after purification on column chromatography.

Last, naphthoyl and furoyl chlorides were improved as reagents to prepare polyheteroaromatic receptors with proflavine leading to compounds **4a** and **4b** with good yields (86 and 70% respectively), as reported in Fig. 3.

The study of the spectral absorption properties showed that the maximal absorption wavelength observed for all the compounds averaged 330 nm. At this absorption wavelength, all the compounds emitted fluorescence at 350 and 400 nm. An example of absorption and fluorescence graphs obtained with compound **2c** is reported in Fig. 4.

3. Pharmacology

The toxicity and phototoxicity of acridine derivatives were evaluated against both transformed Chinese Hamster Ovary Cells (CHO, ATCC) and primary cultures of human keratinocytes. Their corresponding photo-inducible clastogenicity was studied by measuring their capacity to induce chromosome mutations and/or misaggregations, as assessed by the micronucleus assay [15]. Structure–activity relationships were performed in order to better analyze the mechanisms by which acridine derivatives exerted their biological activities. Predictive models were used to

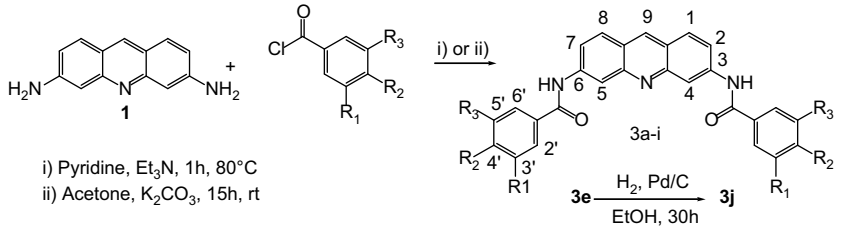

i) Pyridine, Et_3N, 1h, 80°C
ii) Acetone, K_2CO_3, 15h, rt

Comp	R_1	R_2	R_3	Yields	MW	Molecular formula	Mp°C
3a[a,b]	H	H	H	79%	417	$C_{27}H_{19}N_3O_2$	248
3b[a]	H	OMe	H	85%	477	$C_{29}H_{23}N_3O_4$	> 260
3c	H	Cl	Cl	84%	553	$C_{27}H_{15}N_3O_2C_{l4}$	> 260
3d	CF_3	H	CF_3	47%	689	$C_{31}H_{15}N_3O_2F_{12}$	190
3e	H	NO_2	H	57%	507	$C_{27}H_{17}N_5O_6$	> 260
3f[c]	H	Me	H	82%	445	$C_{29}H_{23}N_3O_2$	> 260
3g[a]	H	Cl	H	90%	486	$C_{27}H_{17}N_3O_2C_{l2}$	> 260
3h[a]	H	F	H	96%	453	$C_{27}H_{17}N_3O_2F_2$	> 260
3i	H	CN	H	23%	467	$C_{29}H_{17}N_5O_2$	> 260
3j[d]	H	NH_2	H	26%	447	$C_{27}H_{21}N_5O_2$	238

[a] See reference 13, [b] **3a-e** obtained with acetone, [c] **3f-i** obtained with pyridine, [d] **3j** obtained with EtOH, H_2, Pd/C

Fig. 2. Synthesis of compounds **3a**–**j**.

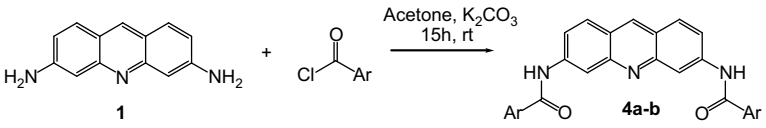

Comp	Ar	Yields	MW	Molecular formula	Mp °C
4a		86%	517	$C_{35}H_{23}N_3O_2$	>260
4b		70%	397	$C_{23}H_{15}N_3O_4$	174

Fig. 3. Synthesis of compounds **4a** and **4b**.

calculate the lipohilicity (log *P*), the solubility (log *S*) and the electrophilicity of the compounds [16]. Then, the experimental data were compared with the antineoplastic, mutagenic and photosensitizer activities predicted by the PASS database [17], according to their chemical similarity with known active molecules.

Finally, in order to better understand the mechanisms by which acridine derivatives exerted their clastogenicity and photo-clastogenicity against CHO cells, the role of oxidative events on the clastogenic effects of compound **2c**, the most photo-inducible clastogenic compound of the series, was investigated in the presence of the protective antioxidant mannitol [18].

4. Results and discussion

Complete data concerning the physicochemical properties and the photo-inducible biological activities of 3,6-di-substituted acridines are summarized in Table 1.

The lipophilicity of each chemical compound was estimated by the prediction of the *n*-octanol/water partition coefficient log *P*, defined as the ratio of concentration in an immiscible solvent such as *n*-octanol to the concentration in the aqueous phase. Results showed that all partition coefficients reported in Table 1 were greater than 1, indicating that proflavine derivatives exhibited lipophilic properties. Nevertheless, the lipophilicity varied according to the nature of the 3,6-substituted groups: compounds bearing aliphatic substituents displayed lower lipophilicity than those bearing aryl rings. As expected, all the acridine derivatives exhibited weak solubility in water. For this reason, the highest tested concentration was 50 μM.

Electrophilicity was expressed as the probability P_e for each compound to initiate electrophilic reactions: acridine analogues were considered electrophilic when $P_e > 0.5$. Results reported in Table 1 showed that P_e greatly varied according to the chemical structure of the compounds. **3d** and **3j** displayed the highest predictive values (0.941 and 0.966 respectively), **2a**, **2e**, **3f** and **3i** were characterized by a moderated electrophilicity, while the other compounds displayed low electrophilic properties.

Predictive values for biological activities were obtained by comparing the chemical structure of each compound with structures or sub-structures of more than 30,000 well-known biologically active drugs. They were expressed as the probability P_a of each compound to be active and illustrated its degree of similarity with well-known antineoplastic compounds, mutagenic molecules, or photosentitizers. $P_a > 0.7$ indicated that the corresponding compound was very likely to reveal activity in experiments, $0.5 < P_a < 0.7$ suggested that the compound was likely to reveal activity in experiments, while $P_a < 0.5$ implied that the compound was unlikely to reveal activity in experiments. All the predictive probabilities calculated for the antineoplastic activity were higher than 0.5: they implied that the 3,6-di-substituted proflavine derivatives were likely to exert cytotoxic activity against tumour cells. Among these compounds, four derivatives (**3h**, **3b**, **3a** and **3e**) showed P_a higher than 0.7. Concerning the mutagenic or the photosensitising activities on the contrary, almost all the estimated P_a were lower than 0.3. They indicated that, according to the predictive model, the 3,6-di-substitued acridines were unlikely to exert mutagenicity or photo-inducible biologic activities.

The cytotoxicity of proflavine derivatives was primarily assessed on transformed Chinese Hamster Ovary cells. In the dark, ten derivatives exerted a significant cytotoxic activity against CHO cells. However, only **2d** displayed a strong cytotoxicity with IC_{50} averaging 0.11 μM, while **4b** and **2f** appeared less active ($IC_{50} = 2.5$ μM and $IC_{50} = 6.1$ μM respectively). These results suggested the important cytotoxic role of the 1,1-dimethylethyl group on the border of the molecules. After UV irradiation on the contrary, almost all the compounds exhibited a significant cytotoxic activity. This photo-enhanced toxicity could be explained by the capacity of the compounds to mainly absorb light rays at 330 nm. Compounds **3a** and **4a** displayed the highest photo-inducible properties, since UV light induced respectively a 90 and 130 fold increase of their cytotoxicity. Nevertheless, **2d** and **2f** remained the most cytotoxic derivatives ($IC_{50} = 0.1$ μM), with cytotoxic activities that did not depend on

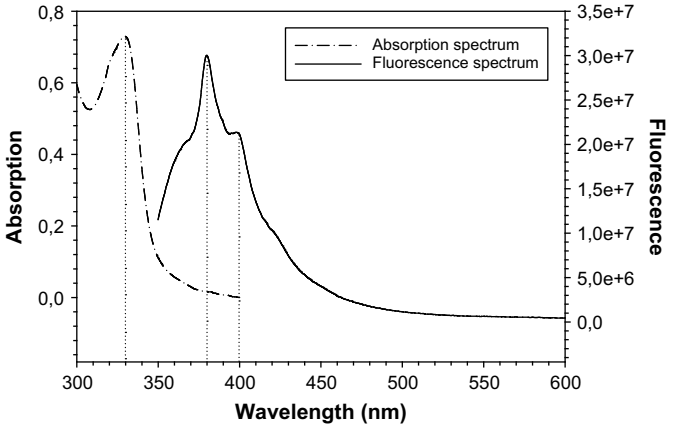

Fig. 4. Absorption and fluorescence spectra of compound **2c**.

Table 1
Photo-inducible cytotoxicity and clastogenicity of proflavine derivatives.

Compounds	Physicochemical properties			Predictive values			Experimental data					
				Biological effects, P_a			Cytotoxicity				Clastogenic activity MCC (μM)	
							CHO cells $IC_{50\text{-}CHO}$ (μM)		Keratinocytes $IC_{50\text{-}kera}$ (μM)			
	log *P*	log *S*	P_e	AntiN	Mut	Photo	− light	+ light	− light	+ light	− light	+ light
1	1.7	−3.5	0.958	0.789	0.481	0.305	1.1	0.52	>50	>50	0.005	0.004
2a	1.9	−4.3	0.809	0.588	0.280	0.266	>50	37.2	>50	41.2	11.01	0.24
2b	2.9	4.7	0.409	0.600	0.160	0.260	>50	2.9	>50	2.4	1.15	0.03
2c	3.9	−4.9	0.208	0.598	0.160	0.260	38.9	1.34	>50	0.57	1.01	0.007
2d	4.5	−5.3	0.137	0.543	0.152	0.254	0.11	0.1	3.28	4.69	NS	NS
2e	2.5	−4.7	0.843	0.642	0.218	0.273	15.8	3.8	>50	8.1	0.47	0.21
2f	5.1	−5.8	0.162	0.578	0.194	0.280	6.1	0.12	>50	0.14	NS	NS
3a	4.9	−6.1	0.567	0.716	0.189	0.281	23.8	0.26	>50	0.33	NS	NS
3b	5.1	−5.9	0.393	0.744	0.179	0.260	45.2	43.41	>50	>50	NS	NS
3c	7.3	−7.9	0.218	0.635	0.196	0.242	>50	>50	>50	>50	NS	NS
3d	8.1	−7.9	0.941	0.608	0.147	0.270	>50	>50	>50	>50	NS	NS
3e	4.8	−6.3	0.281	0.709	0.400	0.236	40.2	>50	>50	>50	NS	NS
3f	5.7	−6.4	0.624	0.613	0.211	0.277	43.1	1.34	>50	4.04	2.11	0.02
3g	6.1	−6.7	0.396	0.658	0.196	0.256	>50	0.94	>50	5.4	2.38	0.12
3h	5.1	−6.3	0.384	0.783	0.140	0.240	>50	>50	>50	>50	NS	1.81
3i	4.9	−6.3	0.743	0.587	0.146	0.257	>50	3.46	>50	33.5	NS	0.06
3j	3.2	−5.8	0.966	0.649	0.320	0.262	>50	>50	>50	>50	NS	0.13
4a	6.8	−7.6	0.474	0.669	0.205	0.276	42.3	0.32	>50	24.1	NS	0.13
4b	3.6	−5.2	0.423	0.538	0.140	0.295	2.5	16.4	34.1	19.3	NS	NS

log *P*: Lipophilicity; log *S*: Solubility; P_e: Electrophilic properties; AntiN: Antineoplastic activity; Mut: Mutagenicity; Photo: Photosensitizer; MCC: Minimal Clastogenic Concentration.

UV irradiation. A significant correlation could be observed between the cytotoxic and the photo-cytotoxic activities against CHO cells ($P = 0.01$). This indicated that, although UV irradiation greatly increased the toxicity of the compounds, the mechanism by which proflavine derivatives may exert a photo-inducible inhibition of cell proliferation was quite similar to those occurring in the dark. However, no correlation could be established between the calculated physicochemical properties of the compounds (lipophilicity, solubility, electrophilicity) and their cytotoxic or photo-cytotoxic activities. Finally, no correlation could be observed between the calculated antineoplastic and the measured cytotoxic properties.

In order to evaluate the specificity of acridine derivatives for rapid growing tumour cells, the cytotoxicity of each compound was also measured on normal human keratinocytes. In the dark, almost all the 3,6-di-substituted acridines, except **2d** and **4b**, were deprived from activity against keratinocytes. After UV irradiation on the contrary, almost all the compounds exerted a significant photo-cytotoxicity. **2c**, **2f** and **3a** displayed the most important photo-inducible properties, with IC_{50} averaging 0.14–0.57 μM and corresponding to a 100 fold increase of their cytotoxicity as compared to experiments performed in the dark. A significant correlation could be observed between the cytotoxicity and the photo-cytotoxicity of 3,6 di-substituted acridines against both CHO cells and human keratinocytes ($P = 0.02$ and $P = 0.001$ respectively). This result implied that a similar mechanism of action occurred in CHO cells and in human keratinocytes. They also focussed on the weak specificity of the compounds for tumour cells, as compared to their parent therapeutic molecule proflavine.

The clastogenic properties of newly synthesized acridines were assessed on Chinese Hamster Ovary cells. In the dark, six derivatives exhibited a significant clastogenic activity. Among them, **2c**, **2b** and **2e** appeared the most clastogenic compounds, with MCC reaching 1.01, 1.15 and 0.47 μM respectively, whereas **3f**, **3g** and **2a** were less active. Acridines that bore aliphatic chains on the 3- and 6-substituted amino groups displayed higher clastogenicity than those bearing aryl rings. This result demonstrated that planar molecules with aliphatic substituents (e.g. **2a**–**f**) could better intercalate between base-pairs than diphenyl substituted molecules **3a**–**j** and focused on the critical role of the steric cluster on DNA–acridine interactions. They also established that the presence of a methyl radical on the border of the substituted groups was determinant for the clastogenic activity. However, all the 3,6-di-substituted acridines were far less clastogenic than the parent molecule proflavine: this indicated that the addition of aliphatic or aromatic substituents on the 3- and 6-amino groups of proflavine greatly decreased the capacity of the molecule to interact with DNA. After UV irradiation, all the derivatives found to be clastogenic in the dark, displayed a higher activity. Moreover, four molecules which were deprived from genotoxicity in the dark revealed a photo-inducible clastogenicity: **3h**, **3i**, **3j** and **4a**. All these compounds, except **4a** contained a single substituent (F, Cl or CN) on position 4 of the aryl rings. No correlation could be established between the cytotoxic and clastogenic activities, suggesting that the interaction of acridines with DNA or with DNA-replication enzymes could not be considered as the single mechanism leading to cell growth arrest. No significant correlation could be found between the calculated electrophilic or mutagenic properties of the compounds and their experimental clastogenicity. Moreover, no significant correlation could be obtained between their calculated photosensitising activity and their photo-inducible clastogenicity. Nevertheless, a significant correlation could be established between the clastogenic and photo-inducible clastogenic effects. This result implied that UV irradiation could enhance the interactions of the compounds with DNA without greatly modifying their mechanism of action.

In order to better visualize the biological effects of acridines on both tumour cells and keratinocytes, a specific cytotoxic power (IC_{50}-CHO/IC_{50}-Kera), a clastogenic power (1/MCC) and a specific photo-induced cytotoxic power were calculated for

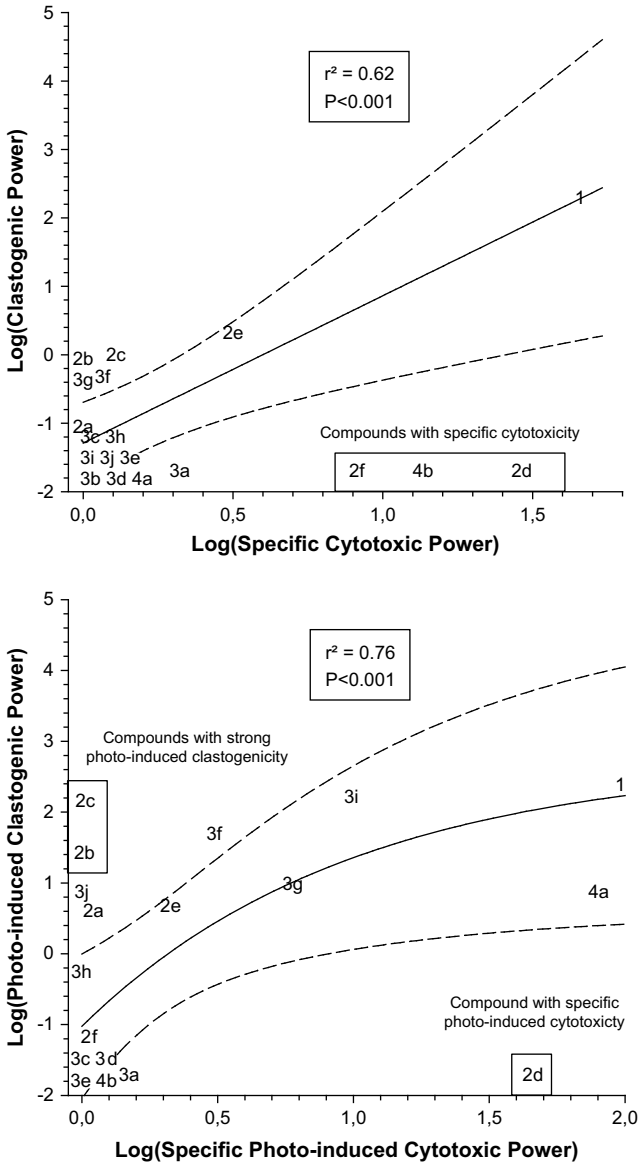

Fig. 5. Schematic representations of the cytotoxic and clastogenic properties in the dark (5.1.) and after irradiation (5.2.).

each acridine derivative and reported in Fig. 5. A significant linear correlation could be observed between the clastogenic power and the specific cytotoxic power for all the compounds except compound **2d**. Similarly, a significant non-linear correlation could be obtained between the photo-induced cytotoxic power and the photo-induced clastogenic power, for all the derivatives except compound **2d**. This result indicated that all the derivatives presented the same mechanisms of action, except compound **2d**, that interfered with different cellular targets.

The clastogenic and photo-enhanced clastogenic effects of **2c** on CHO cells in the presence of mannitol are displayed in Fig. 6. Results showed that mannitol, which significantly decreased by 42% the micronucleated cell rates induced by a high UV irradiation (20 J/cm2, data not shown), did not prevent cells from the clastogenic and photo-enhanced clastogenic activities of compound **2c**. This result indicated that the clastogenic and photo-enhanced clastogenic activities of compound **2c** did not significantly depend on oxidative events.

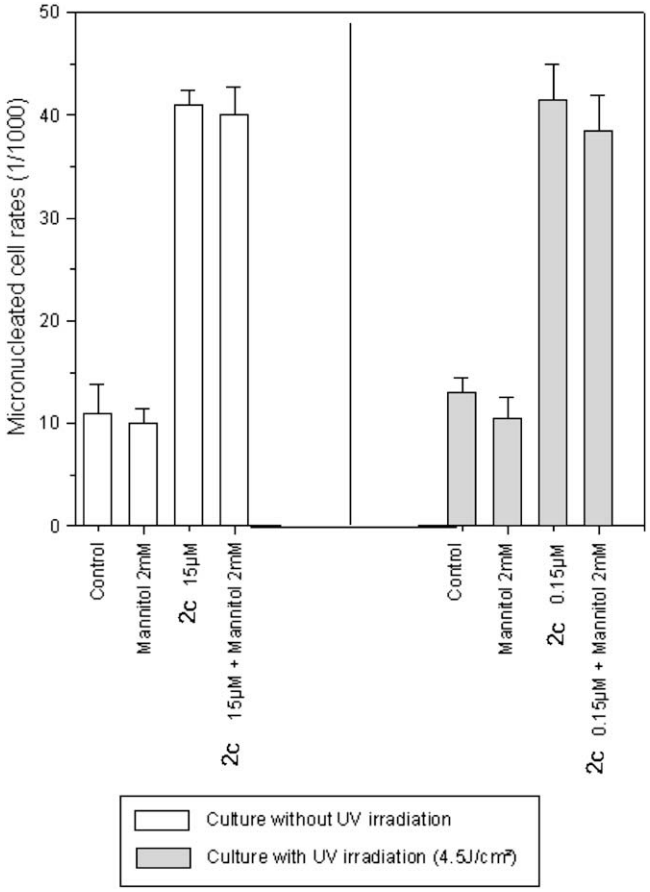

Fig. 6. Combined clastogenic effects of the antioxidant mannitol and compound **2c**.

5. Conclusion

Results observed in this study clearly demonstrated that compound **2d** (*N*-[6-(pivalamino)acridin-3-yl]pivalamide) displayed a specific cytotoxicity on CHO cells and was deprived from significant clastogenicity. They also established that most of the acridine compounds, which have been shown to mainly absorb light rays at a wavelength of 330 nm, could be photo-activated by UVA-visible irradiation. Compound **2c** (*N*-[6-(butyrylamino)acridin-3-yl]butanamide) appeared the strongest photosensitizer, however its genotoxicity and photo-inducible genotoxicity did not depend on oxidative events. This result confirmed our previously published data [13], which showed that compound **2c** directly interacted with DNA through intercalation between base-pairs.

Structure–activity relationships indicated that the presence of a 1,1-dimethylethyl substituent on the positions 3 and 6 of the acridine compounds was responsible for an interesting non-clastogenic and specific cytotoxicity, whereas nonbranched aliphatic chains tended to enhance the ability of the molecules to interfere with DNA. They also demonstrated that compounds bearing nonbranched aliphatic chains could better intercalate between DNA base-pairs than those containing aromatic substituents, and underlined the important role of the steric cluster on DNA–acridine interactions.

Comparisons between the experimental results and the physico-chemical or biological properties calculated by predictive models showed that the cytotoxic and clastogenic activities of acridine compounds resulted from various complex mechanisms. They focussed on the difficulty to properly analyze the

pharmacological properties of acridine derivatives and to predict their biological activities. They also underlined the necessity of extended studies to better define their numerous cellular targets.

6. Experimental

6.1. General procedures

All reagents were of analytical grade, dried and purified when necessary. Proflavine derivatives were dissolved in sterile dimethyl sulfoxide (analytical grade, Sigma) and stored frozen at −70 °C until used. Proflavine (Pro) was used as positive control.

6.2. Mathematical models for prediction of physicochemical and biological properties

Predictive values calculated for lipophilicity (log *P* representing *n*-octanol/water partition coefficient) and solubility in water (log *S*), as well as prediction of acid–base ionization constant pK_a were estimated by mathematical methods using ALOGPS v.2.0 software according to the methodology described by Tetko et al. [19]. Predictive values concerning the electrophilic properties in relation with a possible mutagenic activity were calculated according to the mathematical model developed by Zheng et al. [16], available at the web-server address http://dddc.ac.cn/adme/run.php.

Predictive values for antineoplasic, mutagenic and photosensizer activities were investigated using the chemistry software server PASS for prediction of biological activities spectrum (http://195.178.207.233/PASS/), according to the mathematical model and the database developed by Lagunin et al. [17] and Poroikov et al. [20].

6.3. Chemistry

Melting points were performed on an Electrothermal 9200 melting point apparatus and are uncorrected. The ^{1}H and ^{13}C NMR spectra were measured on a BRUKER AC 300 spectrometer (300.13 MHz for ^{1}H). The mass spectra were performed with a QStar Elite mass Spectrometer (Applied Biosystems SCIEX, Concord, ON, Canada) equipped with an electrospray ionization (ESI) source operated in the positive ion mode. The absorption spectra were performed at a fixed concentration of 1×10^{-5} mg/mL in DMSO with a Perkin–Elmer Lambda 800 spectrophotometer maintained at 25 °C. Fluorescence measurements were achieved with a Horiba–Jobin–Yvon fluoromax-3 spectrofluorimeter equipped with slit widths of 2/2 nm. Fluorescence spectra were obtained by using 1×0.2 cm cells (Hellma), at an excitation wavelength of 330 nm, corresponding to the maximum absorption wavelength for all the compounds.

The proflavine used neutral. Hemisulfate of 3,6-diaminoacridine (proflavine), commercially available, was dissolved into water and NH_4OH 10% was added until pH = 8 under stirring. Then, the solution was filtered, washed with water and the resulting product dried to yield neutral proflavine.

6.3.1. N-*[6-(Acetylamino)acridin-3-yl]acetamide* (***2a***) [13]

Proflavine **1** (300 mg, 1.43 mmol, 1 equ.) and K_2CO_3 (1.98 g, 14.34 mmol, 10 equ.) was dissolved into acetone (40 mL) under N_2. Then, a solution of acetyl chloride (0.31 mL, 4.30 mmol, 3 equ.) into acetone (10 mL) was added dropwise at 0 °C under vigorously stirring. Stirring was continued 15 h more at room temperature. Then, the mixture was poured into a solution of aq. $NaHCO_3$ (40%, 80 mL). After cooling at 5 °C, the obtained precipitate was filtered, washed in water and dried. Recrystallization from ethanol yielded pure **2a** as brown powder. Yield 60%. M.p. > 260 °C. NMR ^{1}H (DMSO-d_6): 10.35 (NH), 8.86 (H_9), 8.49 (H_4 and H_5), 7.59 (H_2 and H_7), 8.03 (H_1 and H_8), 2.15 (Me). ESI-MS: 294 $(M + H)^+$.

6.3.2. N-*[6-(Propionylamino)acridin-3-yl]propanamide* (***2b***) [13]

Proflavine **1** (210 mg, 1 mmol, 1 equ.) was dissolved into pyridine (6 mL) under N_2 and NEt_3 (0.5 mL) was added. Then, propionic anhydride (2.1 mmol, 2.1 equ., 0.27 mL) was added dropwise at 50 °C and stirring was continued for 50 min more at 80 °C. The resulting mixture was poured into water (80 mL) and the obtained precipitate was filtered, washed with water and dried. The resulting solid was recrystallized from ethanol to give an orange powder **2b**. Yield 65%. M.p. > 260 °C. NMR ^{1}H (DMSO-d_6): 10.28 (NH), 8.81 (H_9), 8.48 (H_4 and H_5), 8.01 (H_1 and H_8), 7.60 (H_2 and H_7), 2.43 (CH_2-1′), 1.13 (Me-2′). ESI-MS: 322 $(M + H)^+$.

6.3.3. N-*[6-(Butyrylamino)acridin-3-yl]butanamide* (***2c***) [13]

As reported for **2b** but with butyric anhydride (0.35 mL). The resulting solid was recrystallized from ethanol to give an orange powder **2c**. Yield 32%. M.p. 216 °C. NMR ^{1}H (DMSO-d_6): 10.27 (NH), 8.80 (H_9), 8.50 (H_4 and H_5), 7.98 (H_1 and H_8), 7.58 (H_2 and H_7), 2.38 (CH_2-1′), 1.67 (CH_2-2′), 1.09 (Me). ESI-MS: 350 $(M + H)^+$.

6.3.4. N-*[6-(Pivalamino)acridin-3-yl]pivalamide* (***2d***)

As report for **2a** but with pivaloyl chloride (0.53 mL). A beige powder **2d** was recovered. Yield 74%. M.p. 158 °C. NMR ^{1}H (DMSO-d_6): 9.55 (NH), 8.83 (H_9), 8.52 (H_4 and H_5), 8.02 (H_1 and H_8), 7.79 (H_2 and H_7), 1.30 (Me). ESI-MS: 379 $(M + H)^+$.

6.3.5. *Methyl N-[6-(methoxycarbonylamino)acridin-3-yl]-carbamate* (***2e***) [21]

Proflavine **1** (300 mg, 1.43 mmol, 1 equ.) and $NaHCO_3$ (602 mg, 7.17 mmol, 5 equ.) was dissolved into acetone (15 mL) and methyl chloroformate (1.11 mL, 14.34 mmol, 10 equ.) was added dropwise at room temperature. The solution was stirred for 3 days at 60 °C. Then, the mixture was poured into a solution of aq. $NaHCO_3$ (40%, 80 mL). After cooling at 5 °C, the obtained precipitate was filtered, washed in water and dried. The solid product was finally washed with diethyl oxide (15 mL) and dried to give a brown powder **2e**. Yield 70%. M.p. > 260 °C, (litt. >360 °C) [21]. NMR ^{1}H (CD_3OD): 8.77 (H_9), 8.27 (H_4 and H_5), 7.96 (H_1 and H_8), 7.57 (H_2 and H_7), 3.82 (OMe). ESI-MS: 326 $(M + H)^+$.

6.3.6. Tert-*butyl* N-*[(6*-tert-*butoxycarbonylamino)acridin-3-yl]carbamate* (***2f***) [22]

Proflavine **1** (500 mg, 2.39 mmol, 1 equ.) was dissolved into acetone (63 mL) and di-*tert*-butyl dicarbonate (6.25 g, 28.57 mmol, 12 equ.) was added dropwise at room temperature under N_2. The solution was stirred for 3 days under reflux. The solvent was evaporated in vacuo and the crude product was purified by column chromatography on silica gel (EtOAc/Hexane: 1/1) to yield a yellow powder **2f**. Yield 75%. M.p. 165 °C, (Litt. 163–165 °C) [22]. NMR ^{1}H (DMSO-d_6): 9.80 (NH), 8.76 (H_9), 8.20 (H_4 and H_5), 7.96 (H_1 and H_8), 7.58 (H_2 and H_7), 1.54 (Me). ESI-MS: 411$(M + H)^+$.

6.3.7. N-*[6-(Benzoylamino)acridin-3-yl]benzamide* (***3a***) [13]

Proflavine **1** (300 mg, 1.43 mmol, 1 equ.) and K_2CO_3 (1.98 g, 14.34 mmol, 10 equ.) was dissolved into acetone (40 mL) under N_2. Then, a solution of benzoyl chloride (4.30 mmol, 3 equ.), (0.5 mL) into acetone (10 mL) was added dropwise at 0 °C under vigorous stirring. Stirring was continued 15 h more at room temperature; then the mixture was poured into water (30 mL) and followed by 20 mL of satd. aq. $NaHCO_3$ solution. After cooling at 5 °C, the obtained precipitate was filtered, washed with water, followed by ether (15 mL) and dried to yield an orange powder **3a**. Yield 79%. M.p. 248 °C. NMR ^{1}H (DMSO-d_6): 10.69 (NH), 8.95 (H_9), 8.73 (H_4 and

H_5), 8.13 (H_1 and H_8), 8.05 ($H_{2'}$ and $H_{6'}$), 7.92 (H_2 and H_7), 7.65 ($H_{4'}$), 7.58 ($H_{3'}$ and $H_{5'}$). ESI-MS: 418 $(M+H)^+$.

6.3.8. 4-Methoxy-*N*-[6-(4-methoxybenzoylamino)acridin-3-yl]benzamide (***3b***) *[13]*

As reported for **3a** but with 4-methoxybenzoyl chloride (0.58 mL). **3b** was obtained as a beige powder. Yield 85%. M.p. > 260 °C. NMR ^{1}H (DMSO-d_6): 10.50 (NH), 8.91 (H_9), 8.65 (H_4 and H_5), 8.10 (H_1 and H_8), 8.03 ($H_{2'}$ and $H_{6'}$), 7.89 (H_2 and H_7), 7.09 ($H_{3'}$ and $H_{5'}$), 3.85 (OCH_3). ESI-MS: 478 $(M+H)^+$.

6.3.9. 3,4-Dichloro-*N*-[6-(3,4-dichlorobenzoylamino)acridin-3-yl]benzamide (***3c***)

As reported for **3a** but with 3,4-dichlorobenzoyl chloride (901 mg). **3c** was obtained as an orange powder. Yield 84%. M.p. > 260 °C. NMR ^{1}H (DMSO-d_6): 10.78 (NH), 8.94 (H_9), 8.69 (H_4 and H_5), 8.31 ($H_{2'}$), 8.14 (H_1 and H_8), 8.03 ($H_{6'}$), 7.89 ($H_{5'}$), 7.87 (H_2 and H_7). ESI-MS: 554/556/558 $(M+H)^+$.

6.3.10. 3,5-Di-(trifluoromethyl)-*N*-[6-(3,5-di-(trifluoromethyl)benzoylamino)acridin-3-yl]benzamide (***3d***)

As reported for **3a** but with 3,5-di-(trifluoromethyl)benzoyl chloride (0.78 mL). The resulting crude product was dissolved in methanol (30 mL), filtered and concentrated to yield a brown product **3d**. Yield 47%. M.p. 190 °C. NMR ^{1}H (DMSO-d_6): 11.03 (NH), 8.98 (H_9), 8.71 ($H_{2'}$ and $H_{6'}$), 7.69 ($H_{4'}$), 8.42 (H_4 and H_5), 8.18 (H_1 and H_8), 7.89 (H_2 and H_7). ESI-MS: 690 $(M+H)^+$.

6.3.11. 4-Nitro-*N*-[6-(4-nitrobenzoylamino)acridin-3-yl]benzamide (***3e***)

As reported for **3a** but with 4-nitrobenzoyl chloride (800 mg). The resulting product was washed with diethyl oxide (10 mL) and dried to yield a brown solid **3e**. Yield 57%. M.p. > 260 °C. NMR ^{1}H (DMSO-d_6): 10.97 (NH), 8.97 (H_9), 8.72 (H_4 and H_5), 8.43 ($H_{2'}$ and $H_{6'}$), 8.28 ($H_{3'}$ and $H_{5'}$), 8.15 (H_1 and H_8), 7.91 (H_2 and H_7). ESI-MS: 508 $(M+H)^+$

6.3.12. 4-Methyl-*N*-[6-(4-methylbenzoylamino)acridin-3-yl]benzamide (***3f***) *[23]*

Proflavine **1** (210 mg, 1 mmol, 1 equ.) was dissolved into pyridine (6 mL) under N_2 and NEt_3 (0.5 mL) was added. Then, 4-methylbenzoyl chloride (2.1 mmol, 2.1 equ., 0.40 mL) was added dropwise at 50 °C and stirring was continued for 50 min. more at 80 °C. The resulting mixture was poured into water (80 mL) and the obtained precipitate was filtered, washed with water and dried. Recrystallization from ethanol yielded a brown powder **3f**. Yield 82%. M.p. > 260 °C [23]. NMR ^{1}H (DMSO-d_6): 10.55 (NH), 8.90 (H_9), 8.68 (H_4 and H_5), 8.09 (H_1 and H_8), 8.00 ($H_{2'}$ and $H_{6'}$), 7.91 (H_2 and H_7), 7.43 ($H_{3'}$ and $H_{5'}$), 2.42 (Me). ESI-MS: 446 $(M+H)^+$.

6.3.13. 4-Chloro-*N*-[6-(4-chlorobenzoylamino)acridin-3-yl]benzamide (***3g***) *[13]*

As reported for **3f** but with 4-chlorobenzoyl chloride (0.24 mL). The resulting solid was recrystallized from ethanol to give an orange powder **3g**. Yield 90%. M.p. > 260 °C. NMR ^{1}H (DMSO-d_6): 10.71 (NH), 8.92 (H_9), 8.68 (H_4 and H_5), 8.11 (H_1 and H_8), 8.06 ($H_{2'}$ and $H_{6'}$), 7.89 (H_2 and H_7), 7.66 ($H_{3'}$ and $H_{5'}$). ESI-MS: 486/488 $(M+H)^+$.

6.3.14. 4-Fluoro-*N*-[6-(4-fluorobenzoylamino)acridin-3-yl]benzamide (***3h***) *[13]*

As reported for **3f** but with 4-fluorobenzoyl chloride (0.25 mL). After recrystallization in ethanol, **3h** was obtained as an orange powder. Yield 96%. M.p. > 260 °C. NMR ^{1}H (DMSO-d_6): 10.77 (NH), 9.07 (H_9), 8.76 (H_4 and H_5), 8.16 (H_1 and H_8), 8.13 ($H_{2'}$ and $H_{6'}$), 7.91 (H_2 and H_7), 7.41 ($H_{3'}$ and $H_{5'}$). ESI-MS: 454 $(M+H)^+$.

6.3.15. 4-Cyano-*N*-[6-(4-cyanobenzoylamino)-acridin-3-yl]-benzamide (***3i***)

As reported for **3f** but with 4-cyanobenzoyl chloride (350 mg). The resulting product was washed with hot ethanol (15 mL) and dried to yield a brown solid **3i**. Yield 23%. M.p. > 260 °C. NMR ^{1}H (DMSO-d_6): 10.87 (NH), 8.95 (H_9), 8.71 (H_4 and H_5), 8.20 ($H_{2'}$ and $H_{6'}$), 8.14 (H_1 and H_8), 8.07 ($H_{3'}$ and $H_{5'}$), 7.89 (H_2 and H_7). ESI-MS: 468 $(M+H)^+$.

6.3.16. 4-Amino-*N*-[6-(4-aminobenzoylamino)acridin-3-yl]benzamide (***3j***)

A solution of **3e** (400 mg, 0.79 mmol, 1 equ.) and 10% palladium on carbon (60 mg, 15% wt) in ethanol (40 mL) was prepared. H_2 was introduced into the flask (3 bar) and the reaction mixture was stirred vigorously for 20 h. Then, more ethanol (30 mL) was added and the solution was filtered by passing through Celite. The alcoholic filtrate was concentrated and the resulting crude product was chromatographied on silica gel (DCM/MeOH: 9/1 to 8/2) to yield a red-brown powder **3j**. Yield 26%. M.p. 238 °C. NMR ^{1}H (DMSO-d_6): 10.22 (NH), 8.90 (H_9), 8.67 (H_4 and H_5), 8.07 (H_1 and H_8), 7.93 (H_2 and H_7), 7.83 ($H_{2'}$ and $H_{6'}$), 6.65 ($H_{3'}$ and $H_{5'}$), 5.87 (NH_2). ESI-MS: 468 $(M+H)^+$.

6.3.17. N-*[6-(1-Naphtamino)acridin-3-yl]-1-naphthamide (**4a**)*

As reported for **3a** but with 1-naphthoyl chloride (0.65 mL). The obtained product was washed with hot water (20 mL) followed by diethyl oxide (20 mL). After drying an orange powder **4a** was recovered. Yield 86%. M.p. > 260 °C. NMR ^{1}H (DMSO-d_6): 11.02 (NH), 8.96 (H_9), 8.79 (H_4 and H_5), 8.28 ($H_{8'}$), 8.15 (H_1 and H_8), 8.14 ($H_{4'}$), 8.06 ($H_{5'}$), 7.89 (H_2 and H_7), 7.89 ($H_{2'}$), 7.67 ($H_{3'}$), 7.64 ($H_{7'}$), 7.62 ($H_{6'}$). ESI-MS: 518 $(M+H)^+$.

6.3.18. N-*[6-(Furan-2-carboxamido)acridin-3-yl]furan-2-carboxamide (**4b**)*

As reported for **3a** but with 2-furoyl chloride (0.43 mL). **4b** was obtained as an orange powder. Yield 70%. M.p. 174 °C. NMR ^{1}H (DMSO-d_6): 10.58 (NH), 8.89 (H_9), 8.66 (H_4 and H_5), 8.10 (H_1 and H_8), 8.00 ($H_{4'}$), 7.91 (H_2 and H_7), 7.46 ($H_{2'}$), 6.76 ($H_{3'}$). ESI-MS: 398 $(M+H)^+$.

6.4. Biology

6.4.1. Irradiation procedure

Irradiation of cell cultures was carried out with a solar simulator Suntest CPS+ (Atlas Material Testing Technology BV, Moussy le Neuf, France) apparatus equipped with a xenon arc lamp (1100 W), special glass filters restricting transmission of light below 290 nm and near IR-blocking filter. The irradiance for the photoactivation of acridine derivatives was fixed at 750 W m^{-2} throughout the experiments and the combined light dose was 4.5 J/cm^2 for one minute irradiation, corresponding to 0.36 J/cm^2 for UVA and 4.14 J/cm^2 for visible light. The temperature of the samples was kept at 4 °C using a water cooling circuit in the irradiation chamber. UVA–visible light (320–800 nm) was obtained using the solar ID65 filter plus a window glass filter.

6.4.2. Photo-inducible antiproliferative activity on Chinese Hamster ovary cells and human keratinocytes

Chinese Hamster Ovary cells (CHO) were maintained in Mc Coys' 5A medium (Sigma, St Quentin-Fallavier, France) containing 10% foetal calf serum (Eurobio, Paris, France), 2 mM glutamine and penicillin–streptomycin (100 U mL^{-1}–10 μg mL^{-1}). Human normal keratinocytes were isolated from infant foreskin obtained after circumcisions according to the technique described by Decome et al. [24]. Cells were suspended in K-SFM medium containing

25 μg/mL BPE and 0.1–0.2 ng/mL rEGF. Under these conditions, pure keratinocyte cultures were obtained within 2 weeks. CHO and keratinocyte cultures were incubated at 37 °C in humidified atmosphere containing 5% CO_2 and the culture mediums were changed every 3 days.

The effects of acridines on the growth of CHO cells (ATCC, Manassas VA, USA) were assessed by the colorimetric determination of cell viability using the oxidation–reduction indicator WST1®. Non-confluent CHO cells (50,000 by well) were diluted in Mc Coys' 5A medium (Sigma, St Quentin-Fallavier, France) containing 10% foetal calf serum (Eurobio, Paris, France), 2 mM glutamine and penicillin–streptomycin (100 U mL^{-1}–10 μg mL^{-1}) and seeded in 96-well plates. After a 24 h incubation period at 37 °C with 5% CO_2, a range of acridine concentrations was incorporated in duplicate cultures (final DMSO concentration less than 0.5%). Cells were immediately irradiated and incubated for 24 h at 37 °C. At the end of the incubation period, cultures were rinced by three successive washes in Phosphate Saline Buffer (PBS) and incubated for 20 min in RPMI medium without phenol red containing 10% of the oxidation–reduction indicator WST1® at 37 °C. Cell viability was evaluated by the assessment of WST1 absorbance at 450 nm in a microplate spectrophotometer MRX® II (Dynex technologies, VA, USA). $IC_{50\text{-}CHO}$ was defined as the concentration of acridine required to induce a 50% decrease of cell growth, corresponding to a 50% reduction of WST1® indicator as compared to the control culture.

6.4.3. Photo-inducible clastogenic activity on CHO cells

The micronucleus assay was performed according to the methodology recommended by Kirsch-Volders et al. [25]. A total of 50,000 Chinese Hamster Ovary cells (CHO-K1, ATCC) were plated in chamber slides containing Mc Coy's 5A medium (Sigma, St Quentin-Fallavier, France) supplemented with 10% foetal calf serum, 1 mM glutamine and penicillin–streptomycin (100 U mL^{-1}–10 μg mL^{-1}) and were incubated at 37 °C in humidified atmosphere containing 5% CO_2. After a 24 h incubation period, two sets of experiments were performed: a range of acridine concentrations was incorporated in duplicate cultures maintained in the dark, an other range of acridine concentrations was incorporated in duplicate cultures and immediately irradiated. Cells were incubated at 37 °C during 3 h, then culture medium was removed and cells were incubated in fresh medium containing 5 μg mL^{-1} cytochalasin B to arrest cytokinesis. After an additional 24 h incubation period at 37 °C, the culture medium was removed; cells were submitted to two successive washes with PBS and fixed with methanol (HPLC purity grade solvent). Staining of air-dried slides was performed with 5% Giemsa stain in Milli-Q water for 20 min. Slide analysis was performed microscopically at 1000× magnification.

The Proliferative Index (PI) was considered as a measure of cytotoxicity. It was determined by scoring the number of multinucleated cells among 500 Giemsa-stained cells with well-preserved cytoplasm and was calculated as follows:

$$PI = \frac{[MNC + 2 \times (BNC) + 3 \times (TNC)]}{500}$$

With:

MNC: number of cells containing one nucleus
BNC: number of cells containing two nuclei
TNC: number of cells containing three nuclei at least.

The micronucleated cell (MNC) rates were determined for concentrations inducing less than 50% toxicity: for each concentration, 2000 binucleated cells were examined and micronuclei were identified according to the morphological criteria previously defined by Kirsch-Volders et al. [25]. Statistical differences between controls and treated samples were performed by the χ^2-test: a significant clastogenic activity was detected when a dose-dependent increase of micronucleated cells was observed and when the induced micronucleated cell rates were significant for one concentration at least. For each acridine, a dose–effect relationship was calculated by non-linear regression analysis using the TableCurve software (Jandel Scientific Software, San Rafael, CA, USA). The minimal clastogenic concentration (MCC) was defined as the lowest acridine concentration capable to induce a significant increase of the number of micronucleated cells.

*6.4.4. Clastogenic effects of compound **2c** on CHO cells pre-treated with mannitol*

A total of 50,000 Chinese Hamster Ovary cells (CHO-K1, ATCC) were plated in chamber slides containing Mc Coy's 5A medium (Sigma, St Quentin-Fallavier, France) supplemented with 10% foetal calf serum, 1 mM glutamine and penicillin–streptomycin (100 U mL^{-1}–10 μg mL^{-1}) and were incubated at 37 °C in humidified atmosphere containing 5% CO_2. After a 24 h incubation period, 2 mM mannitol was added in cell cultures and cells were incubated at 37 °C for 2 h. Then, three sets of experiments were performed:

- control cultures and cultures containing 2 mM mannitol were submitted to a 20 J/cm^2 irradiation, in order to verify the protective effect of mannitol against the genotoxic effects of UVA light,
- control cultures and cultures containing 2 mM mannitol were treated with 15 μM of compound **2c** and were maintained in the dark,
- control cultures and cultures containing 2 mM mannitol were treated with 0.15 μM of compound **2c** and were submitted to a 4.5 J/cm^2 irradiation.

Cells were incubated at 37 °C during 3 h, then culture medium was removed and cells were incubated in fresh medium containing 5 μg mL^{-1} cytochalasin B to arrest cytokinesis. After an additional 24 h incubation period at 37 °C, the culture medium was removed; cells were submitted to two successive washes with PBS and fixed with methanol (HPLC purity grade solvent). Staining of air-dried slides was performed with 5% Giemsa stain in Milli-Q water for 20 min. Slide analysis was performed microscopically at 1000× magnification.

6.5. Statistical analysis

The rank correlation test of Spearman was used for studying coupled variables. Analysis was performed by Statgraphics plus software (Statistical graphics corporation, USA).

References

[1] W.A. Denny, Curr. Med. Chem. 9 (2002) 1655–1665.
[2] M. Wainwright, J. Antimicrob. Chemother. 47 (2001) 1–13.
[3] I. Antonin, Curr. Med. Chem. 9 (2002) 1701–1716.
[4] M. Demeunynck, A. Charmantray, A. Martelli, Curr. Pharm. Des 7 (2001) 1703–1724.
[5] L.S. Lerman, J. Mol. Biol. 3 (1961) 18–30.
[6] Z. Topcu, J. Clin. Pharm. Ther 26 (2001) 405–416.
[7] L.S. Ripley, A. Clark, Proc. Natl. Acad. Sci. U.S.A. 83 (1986) 6954–6958.
[8] A. Nasim, T. Brychcy, Mutat. Res. 65 (1979) 261–288.
[9] L.R. Ferguson, W.A. Denny, Mutat. Res. 258 (1991) 123–160.
[10] M. Wainwright, D.A. Phoenix, J. Marland, D.R. Wareing, F.J. Bolton, J. Antimicrob. Chemother. 40 (1997) 587–589.
[11] W.J. Firth, S.G. Rock, B.R. Brown, L.W. Yielding, Mutat. Res. 81 (1981) 295–309.
[12] Y. Iwamoto, L.R. Ferguson, A. Pearson, B.C. Baguley, Mutat. Res. 268 (1992) 35–41.

[13] C. Di Giorgio, K. Shimi, G. Boyer, F. Delmas, J.P. Galy, Eur. J. Med. Chem. 42 (2007) 1277–1284.
[14] A. Miloudi, D. El Abed, G. Boyer, J.P. Galy, Heterocycles 68 (2006) 2595–2605.
[15] R. Fenech, Mutat. Res. 285 (1993) 35–44.
[16] M. Zheng, Z. Liu, C. Xue, W. Zhu, K. Chen, X. Luo, H. Jiang, Bioinformatics 22 (2006) 2099–2106.
[17] A. Lagunin, A. Stepanchikova, D. Filimonov, V. Poroikov, Bioinformatics 16 (2000) 747–748.
[18] C. Botta, C. Di Giorgio, A.S. Sabatier, M. De Méo, J. Photochem. Photobiol., B 25 (2008) 24–34.
[19] I.V. Tekto, Y. Tanchuk, A. Villa, J. Chem. Inf. Comput. Sci. 41 (2001) 1407–1421.
[20] V.V. Poroikov, D. Filimonov, Y. Borodina, A. Lagunin, A. Kos, J. Chem. Inf. Comput. Sci. 40 (2001) 1349–1355.
[21] A. Lorente, M. Fernandez-Saiz, J.-F. Espinosa, C. Jaime, J.-M. Lehn, J.-P. Vigneron, Tetrahedron Lett. 36 (1995) 5261–5264.
[22] A. Lorente, Y.-G. Vazquez, M.-J. Fernandez, A. Ferrandez, Biorg. Med. Chem. 12 (2004) 4307–4312.
[23] K. Shimi, G. Boyer, R. Faure, J.-P. Galy, Magn. Reson. Chem. 43 (2005) 1077–1079.
[24] L. Decome, M.P. De Meo, A. Geffard, O. Doucet, G. Dumenil, A. Botta, J. Photochem. Photobiol. B 79 (2005) 101–108.
[25] M. Kirsch-Volders, T. Sofuni, M. Aardema, S. Albertini, D. Eastmond Fenech, M. Ishidate, S. Kirchner, E. Lorge, T. Morita, H. Norppa, J. Surrales, A. Vanhauwaert, A. Wakata, Mutat. Res. 540 (2003) 153–163.